

Medical Image Segmentation Using Information Extracted from Deformation

Kai Xiao
 Shanghai Jiao Tong University
 800 Dong Chuan Road
 Shanghai, 200240, China
 Email: showkey@gmail.com

About Ella Hassanien
 Cairo University
 5 Ahmed Zewal St.
 Orman, Giza, Egypt
 Email: Aboitcairo@gmail.com

Neveen I. Ghali
 Faculty of Science
 Al-Azhar University
 Cairo, Egypt
 Email: nev_ghali@yahoo.com

Abstract—Deformation of normal structures in medical images has usually been considered as undesired and even a challenging issue to be tackled in medical image segmentation and registration tasks. With the objective of improving brain tumor segmentation accuracy in human brain magnetic resonance (MR) images, this paper proposes an approach to extract useful information from the correlation between lateral ventricular deformation and tumor. In some cases, comparative experiments show the improved tumor segmentation accuracy when the extracted information is added as an additional feature.

I. INTRODUCTION

BRAIN tumor segmentation in magnetic resonance (MR) image is an important image processing step for both medical practitioners and scientific researchers. Large amounts of research efforts have been made in developing effective segmentation methods in the past years, however, such methods have failed to achieve the accuracy level comparable to analyses performed by human experts [1], [2], [3], [4].

One of the most challenging problems that hinder the development of accurate automatic systems is that MR image lacks strong association between actual anatomical meaning and MR imaging (MRI) intensity, especially for pathology such as brain tumor. Therefore, in addition to intensities, other features which are relevant to anatomical meaning are necessary for more accurate tumor segmentation.

This paper brings forward the idea of utilizing brain lateral ventricular deformation, which has been normally considered as undesired and challenging, as an additional information for tumor segmentation, and proposes to quantify the deformation information as a feature with a design and implementation of a feature extraction component. The created feature data is then incorporated for improving tumor segmentation accuracy.

II. BACKGROUND

A. Brain Lateral Ventricles and Tumor

A ventricle is an internal cavity of brain. A normal brain contains a connecting system of ventricles, commonly referred to as the ventricular system, which is filled with cerebrospinal fluid (CSF) [5], [6], [7], [8]. Fig. 1 illustrates scans from sequences of T1- and T2-weighted MR images in axial view where lateral ventricles are located in the brain center. Lateral

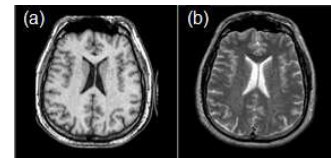


Fig. 1. healthy (a) T1- and (b) T2-weighted brain MR image slices in axial view showing the lateral ventricles, images courtesy of [10].

ventricles are the biggest structures that mainly contain CSF in the axial view of the brain center [9].

As can be seen clearly from Fig. 2(a-i), in cases where brain tumors exist, one or two of the lateral ventricles are compressed; whereas for a healthy brain the two lateral ventricles are nearly symmetrical to each other (see Fig. 1). Fig. 2(j) illustrates the direction of compression from brain tumor and the deformed lateral ventricle. It can be seen that, in some cases, lateral ventricle is compressed in the opposite direction of the location of the brain tumor. This suggests the strong correlation between the two structures. However, due to the fact that brain tumours vary substantially in their location and size, and have diverse effects on lateral ventricles, it is not always the case that brain tumour and deformed lateral ventricles appear in the same image plane. Fig. 3 illustrates how this correlation becomes clear when seen from different planes. The positions of the deformed parts of the lateral ventricle in Fig. 3 (c) and (d) are basically the same as that of the brain tumor in Fig. 3 (b). Fig. 3 (a) illustrates the compression caused by a brain tumour on one lateral ventricle (coronal view). It can be seen that correlations between lateral ventricular deformation and the brain tumor still exist, even though it may not be observable in the same plane or view of MR images.

B. Brain Tumor Segmentation with Lateral Ventricular Deformation

Automatic MR image segmentation systems are typically designed as a combination of several components of pre-processing, feature extraction, segmentation and classification [1]. Feature extraction component which creates relevant data sets is the key to successful segmentation [1]. It can be assumed that, if the correlation between lateral ventricular

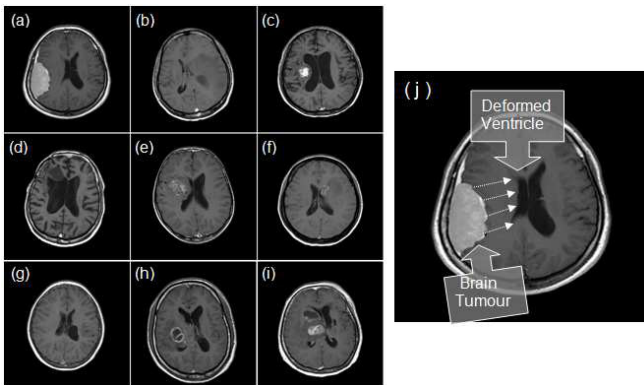


Fig. 2. (a-i): Nine axial view MR image slices from different patients showing brain tumor and lateral ventricles; (j): zoomed illustration of a deformed lateral ventricle and a tumor.

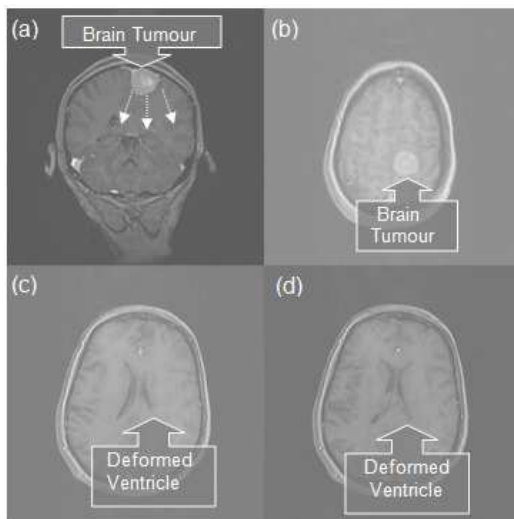


Fig. 3. Some selected MR image slices of one patient showing brain tumour and deformed lateral ventricles not in the same plane of axial view [11]: (a) coronal view in middle of the head; (b) axial view from slice near the top area of the head; (c) axial view from slice in the middle area of the head; (d) axial view from slice next to (c).

deformation and tumor is correctly quantified and used, tumor segmentation accuracy will be accordingly improved.

The fact that lateral ventricles constitute one of the major structures with sharp boundaries in the brain allows for their shapes to be easily delineated from their associated MR images [12], [7], [8]. This makes the feature extraction process based on deformation of this structure relatively more reliable. As a result, lateral ventricular deformation caused by the presence of brain tumors provides an intuition that one could exploit the information derived from the correlations between them. By utilizing this derived information, brain tumor segmentation could be improved.

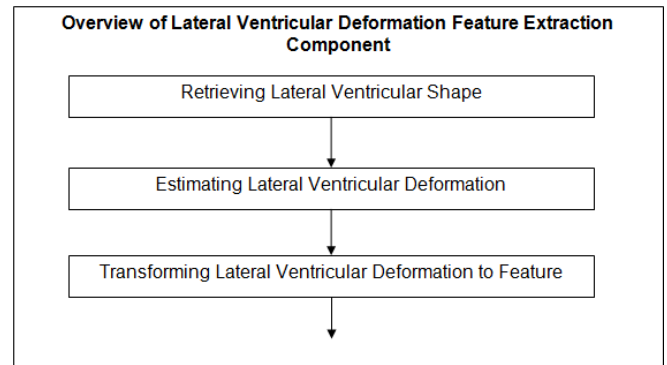


Fig. 4. Overview of the lateral ventricular deformation feature extraction component.

III. DEFORMATION INFORMATION EXTRACTION

A. Overview

The task of extracting the lateral ventricular deformation information should include retrieval of lateral ventricular shape, and transformation of lateral ventricular deformation into feature. To achieve the latter, one process to model and estimate the deformation of the retrieved lateral ventricular shape should be applied.

The step of modeling and estimating lateral ventricular deformation is to associate template and deformed lateral ventricles, and to model, calculate and quantify shape variation. Hence, both healthy and deformed lateral ventricles must be available for shape comparison. However, lateral ventricles of one person are subject to shape variation with age, even with the absence of pathology or abnormality [13]. Furthermore, because of the varieties of size, location and type of brain tumors [14], [15], [16], their compression effects on lateral ventricles are significantly diverse. There are no lateral ventricles that can be used as a general template to perfectly associate the deformed lateral ventricles in all cases. Therefore, an additional step of adjusting feature data is necessary in the lateral ventricular deformation feature extraction component. The design of lateral ventricular deformation feature extraction component actually consists of the three streamlined processes as illustrated in Fig. 4.

B. Retrieving Lateral Ventricular Shape

The existing works on brain lateral ventricular shape retrieval generally apply the approach of discriminating tissues of ventricles through the analysis on its intensity and geometric location [17], [18]. In this paper, the lateral ventricular shape retrieval is achieved through three steps: brain MR image tissue segmentation for separating CSF tissue from other tissues, CSF identification for locating the image pixels/regions of which lateral ventricles are composed and lateral ventricles extraction for removing CSF pixels outside the lateral ventricular regions.

In order to separate CSF from other tissues, we can create several clusters by applying a clustering method. In this step, brain tissues are clustered according to the similarity of

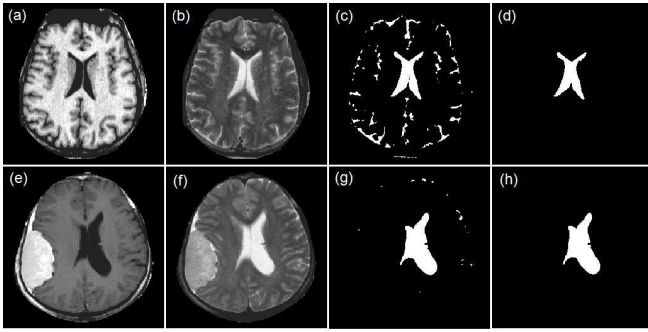


Fig. 5. Lateral ventricular shape retrieval results: (a) healthy T1-weighted MR image data; (b) T2-weighted MR image data of (a); (c) after tissue segmentation on (a) and (b); (d) extracted lateral ventricles from (c); (e) tumor-affected T1-weighted MR image data; (f) T2-weighted MR image data of (e); (g) after tissue segmentation on (e) and (f); (h) extracted lateral ventricles from (g).

MRI intensity of tissue types, and one of the output clusters accommodates CSF tissue. This research applies our previous work of feature-weighted Fuzzy C-Means (fwFCM) [19], [20] which provides higher insensitivity to noise and capability of adjusting feature weights. These properties make fwFCM more suitable for MR images than conventional FCM algorithm.

After brain tissue segmentation, CSF extraction can be conducted by selecting the cluster labeled as CSF from the multiple clusters created by the fwFCM method. It can be seen from Fig. 1 that, under the situation of absence of certain types of lesions, within several major tissue types, CSF is the only one that appears bright in T1-weighted and dark in T2-weighted MR images [6]. As a result, intensity values of CSF in T2-weighted MRI are high while those in T1-weighted MRI are low. This selection process can be expressed as: $\max_i \{V_{T2,i} - V_{T1-i}\}$, where i is the cluster number, V_{T2} and V_{T1} represent the centroid values in the T2- and T1-weighted features respectively in the input feature set of the fwFCM clustering.

Although from brain MR images of axial view, lateral ventricles are of large volume, CSF can still fall outside the ventricular system [6]. Furthermore, the proposed brain tissue segmentation step may wrongly assign non-CSF pixels to the cluster of CSF. To remove undesired pixels, a global mask is applied to remove pixels outside the area where pixels of lateral ventricles normally reside, thereby leaves the regions as the extracted lateral ventricles. Fig. 5 demonstrates the lateral ventricles extraction results by applying this approach.

C. Estimating Lateral Ventricular Deformation

The process of estimating lateral ventricular deformation can be decomposed into two steps: lateral ventricles alignment and lateral ventricular deformation measurement. Lateral ventricles alignment is achieved by two sub-steps of linking lateral ventricles and selecting landmark points. The lateral ventricular deformation measurement step is also achieved by two sub-steps of modeling lateral ventricular deformation and calculating estimated deformation.

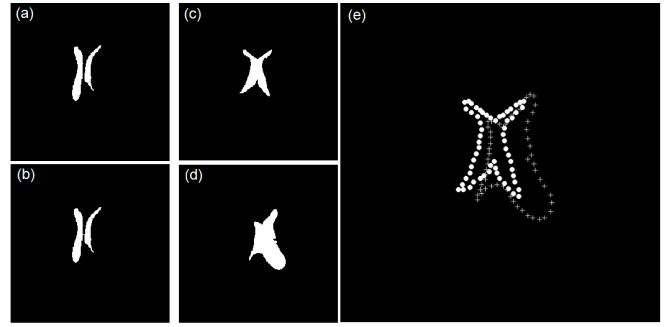


Fig. 6. Lateral ventricles linking and alignment results: (a) separated left and right lateral ventricles; (b) linked left and right lateral ventricles; (c) template; (d) target; (e) aligned template and target. White circles and grey cross represents control points on template and target lateral ventricles, respectively.

In MR images, left and right lateral ventricles are actually separated [7], [8]. Furthermore, lateral ventricles may be broken. To effectively estimate deformation using modeling functions, left and right lateral ventricles are treated as one single object. Therefore left and right ventricles and the disjointed parts of lateral ventricles need to be linked together. Fig. 6(a, b) demonstrate a sample resultant image after the separated lateral ventricles are linked together through a connecting line with the shortest distance.

Based on the study of anatomical properties of brain lateral ventricles, anterior and posterior horns are employed as key landmark points. The process of lateral ventricles alignment is completed by selecting intermediate landmark points based on these key landmark points. Fig. 6(c, d) show the extracted template and target lateral ventricles, respectively. Fig. 6(e) displays the alignment results by selecting the landmark points and overlapping them in one image. However, misalignment effect caused by the applied imperfect template can be easily observed.

Deformation is usually modeled and represented as a transformation function [21]. Generally, in order to model deformation, both linear and non-linear functions can be used. However, with regards to brain MR images, linear transformation functions, cause the images to be globally smoothed, thereby accommodating only very small and simple deformations [22] and making the process of employing them for modeling deformation undesirable. As a nonlinear deformation modeling function, thin plate splines (TPS) function is employed to perform the nonlinear mapping between template and target lateral ventricular boundary image data set [23]. A TPS $f(x, y)$ is a smoothing function which interpolates a surface that is fixed at landmark points P_i at a specific height. TPS can be treated as a process of finding a function $z(x, y)$ which minimizes the bending energy [23], [24]. In the application for 2-dimensional images, instead of assuming that f corresponds to a displacement orthogonal to the image plane at the landmark points, one can treat it as a displacement in the image plane [24]. By using two separate TPS functions f_x and f_y which model the displacement of the selected landmark points in the x and y direction, a vector-valued function F which maps each

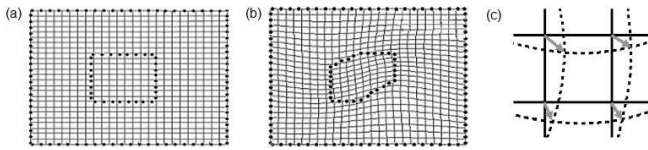


Fig. 7. Example of landmark points with original and deformed TPS meshes formed by x and y coordinates: (a) original; (b) deformed. (c) Illustration of the effect of deformation in a zoomed view before and after deformation, solid and dashed lines are segments of the meshes from the original and deformed image, respectively; grey arrows indicate the vector of the displacement due to deformation.

point of the image into a new point in the image plane can be represented using $(x', y') \rightarrow (f_x(x, y), f_y(x, y))$, where f_x and f_y are the functions causing displacement on x and y coordinates respectively.

Once the vector-valued function F is defined via the selected landmark points with TPS functions, it is then applied to the original coordinates of all pixels in the target image to retrieve new coordinates for all pixels. If one treats some selected horizontal and vertical lines of equal spaces in the original image as a mesh, then a corresponding distorted mesh can be used to describe the displacement of each node of the mesh. This effect is illustrated in Fig. 7(a, b) by visualizing the original and its corresponding deformed meshes after TPS function is applied to all pixels in the image. The effect of the deformation on the lateral ventricles can then be represented by finding out the coordinate displacement value of each pixel in the image. In the deformed image, each pixel is displaced from its original coordinate at specific direction and distance. Therefore, vector can be used for representing the estimated deformation of each point. Fig. 7(c) illustrates an example on a segment of an image using magnitude and direction of vectors to represent the deformation measurement.

D. Transforming Lateral Ventricular Deformation to Features

The process of transforming lateral ventricular deformation to features can be decomposed to two indispensable steps: estimated deformation data to feature conversion and lateral ventricular deformation data adjustment.

The estimated deformation data is normalized to the format of image grayscale value of 8 bits, which can be represented as Equation $I_k = \frac{D_k}{\max\{D\}} \times 255$, where I is the normalized intensity value, k is the index of pixel in the image and 255 is the maximum 8 bits grayscale value of MR image pixels, and D is the magnitude of displacement vector which can be calculated by using the Euclidean distance as $D = \sqrt{(P_{o_x} - P_{t_x})^2 + (P_{o_y} - P_{t_y})^2}$, where P_{o_x} and P_{o_y} are the original data point x and y coordinate values, while P_{t_x} and P_{t_y} are the obtained data point x and y coordinate values, respectively.

It can be seen in Fig. 8(b) that that the maximum measured deformation value is not in the area where tumor resides, and the direction of vector denoting the highest displacement value is irrelevant to that of the compression from the brain tumor. This is mainly because of the misalignment between

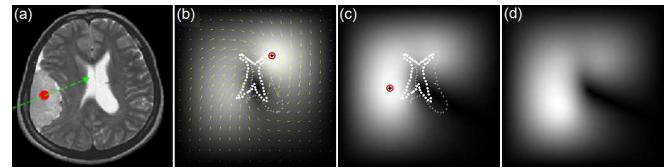


Fig. 8. Example of estimating lateral ventricular deformation: (a) manual selection of tumor, where round dot is selected by user input; (b) visualized deformation estimation, where magnitude of displacement vector is normalized and visualized as image grayscale value, arrows are showing the directions of displacement vectors, and a cross covered by a circle indicates the maximum displacement vector magnitude; (c) visualized deformation estimation; (d) deformation feature extraction final result.

the template and target lateral ventricles caused by using the imperfect lateral ventricles template (as seen in Fig. 6(e)). To address this problem, as shown in Fig. 8(a), a method for adjusting the estimated deformation data is proposed. The method allows user to select one point in the brain tumor. With this reference point, a line can be drawn from the point to the center of the image, at the direction from the border to the center of the image. Deformation estimation values can therefore be adjusted by $D' = D |\cos(\frac{\theta}{2})|$, where D and D' are the magnitudes of the original and adjusted displacement vector representing the estimated deformation, respectively. θ is the angle between the connecting line and the displacement vector. It can be seen that when $\theta = \pi$ (the connecting line and the displacement vector are in the opposite directions), adjusted displacement vector magnitude is reduced to 0. And when $\theta = 0$, magnitude of the adjusted displacement vector is 1, which means the estimated data is kept without any change.

Fig. 8(c) visualizes the estimated deformation data by normalizing it into grayscale values and Fig. 8(d) illustrates the final feature data of lateral ventricular deformation. It can be seen that, although not perfect, the bright area which indicates the high deformation values is approximately in the same location as brain tumor in the original image. The deformation estimation values can then be used as an additional feature in the feature set the brain MR image tumor segmentation methods that support input data of multiple features.

IV. BRAIN TUMOR SEGMENTATION WITH LATERAL VENTRICULAR DEFORMATION FEATURE

A. System Implementation

Structure of the brain tumor segmentation system in this research follows the common MR image segmentation system [1] shown in Fig. 9(a). To investigate the effect of brain tumor segmentation caused by the feature of lateral ventricular deformation, special considerations have to be given to the inclusive components of pre-processing, feature extraction and brain tumor segmentation.

The pre-processing component in this brain tumor segmentation system will need to address the issues of intensity non-standardization, geometrical non-uniformity and redundant data in the image background and skull. These issues are respectively addressed by the four streamlined processes of

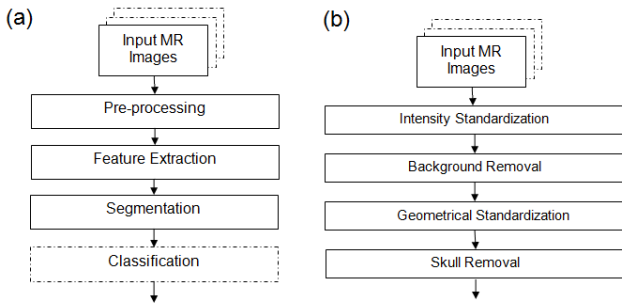


Fig. 9. System structures: (a) structure of a common MR image segmentation system.; (b) overview of the pre-processing component.

intensity standardization, geometrical standardization, background and skull removal processes, as illustrated in Fig. 9(b).

In the segmentation component, selected supervised and unsupervised segmentation methods are used to evaluate the effect of lateral ventricular deformation feature on brain tumor segmentation. In order to achieve that, this research uses two feature sets, one includes the extracted lateral ventricular deformation feature, and the other does not. By comparing the segmentation results using the same segmentation method, i.e., supervised or unsupervised, effectiveness of the feature of brain lateral ventricular deformation can be examined. In this paper, the most frequently used k -nearest neighbors (k -NN) [25], [26], [1] and conventional FCM [27], [19], [20] are selected as supervised and unsupervised methods, respectively. The intention of selecting conventional FCM method is to evaluate the segmentation results by the original segmentation method with no interference or adjustment.

B. Experimentation and Evaluation

To use the supervised k -NN algorithm on brain tumor segmentation, tumor segmentation results from medical experts are used as training samples in which tumor areas are marked. Therefore all pixels in the images can be labeled as tumor or non-tumor. After the k -NN classification, each testing image pixel is categorized as tumor or non-tumor. In the experiments using unsupervised FCM algorithm, the number of clusters is set to 6 denoting six clusters of major brain tissues. The cluster of tumor will be identified manually out from 6 clusters after the clustering process due to the fact that there is no training data for the FCM method.

By using input feature set with or without the extracted deformation feature, pixels segmented as tumor which are in the same class as the corresponding pixels in the segmentation by medical expert are treated as correctly segmented tumor pixels; those segmented as tumor but labeled as non-tumor in the segmentation by medical expert are treated as wrongly segmented tumor pixels.

Statistical measures of sensitivity and specificity [28], [29] are applied for evaluating the segmentation results. By treating correctly segmented tumor, wrongly segmented tumor, correctly segmented non-tumor and wrongly segmented non-tumor pixel number as true positive ($true^+$), false positive

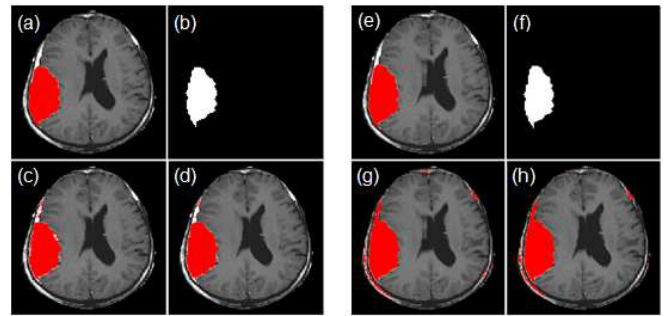


Fig. 10. Training data and tumor segmentation results using k -NN classifier: (a) segmentation by medical expert; (b) training data converted from (a); (c) segmentation result without deformation feature; (d) segmentation result with deformation feature, and segmentation results using FCM clustering method: (e) segmentation by medical expert; (f) visualized segmentation by medical expert; (g) segmentation result without deformation feature; (h) segmentation result with deformation feature.

($false^+$), true negative ($true^-$) and false negative ($false^-$) number respectively, sensitivity and specificity values can be obtained according to: $Sensitivity = \frac{true^+}{true^+ + false^-}$ and $Specificity = \frac{true^-}{true^- + false^+}$, respectively. A sensitivity of 100% means that the test recognizes all actual positives, i.e., all brain tumor pixels are segmented as tumor. And a specificity of 100% means that the test recognizes all actual negatives, i.e., all non-tumor pixels are segmented as non-tumor [28].

The brain tumor segmentation result of one image case is illustrated in Fig. 10. It can be seen from Fig. 10 (d, h) that, the classification results obtained from the feature set with lateral ventricular deformation feature are respectively closer to the results from medical expert than the result shown in Fig. 10 (c, g), which is created from the feature set without lateral ventricular deformation feature.

With more image cases, sensitivity and specificity values tabulated in Table I and Table II provide further evidence of the positive effect from the additional feature. It can be seen from in Table I that from the experiments using supervised k NN, with the inclusion of the extracted lateral ventricular deformation feature, specificity values in the increase for all eight cases. Except for the decrease in case number 3, sensitivity values increase in 7 out of 8 cases. In the experiments using unsupervised FCM as illustrated in Table II, with the inclusion of the extracted lateral ventricular deformation feature, specificity values increase for all eight cases. However, sensitivity values decrease in 3 out of 8 cases. This is mainly because there is no specific rule created for distinguishing between tumor and non-tumor pixels in clustering [30]. In short, the clusters of tumor or non-tumor are not well defined concepts if no training process is included in the segmentation.

V. CONCLUSION

This paper establishes and implements the idea of utilizing deformation of lateral ventricles for brain tumor segmentation. The results show that the extracted lateral ventricular deformation information is relevant to the position of brain tumor.

TABLE I
SPECIFICITY AND SENSITIVITY VALUES OF BRAIN TUMOR SEGMENTATION USING SUPERISED k NN METHOD

	Specificity		Sensitivity	
	Feature Set			
	without deformation	with deformation	without deformation	with deformation
Case 1	99.9%	100.0%	94.3%	95.3%
Case 2	99.9%	100.0%	90.9%	98.2%
Case 3	99.8%	99.9%	95.3%	94.3%
Case 4	99.1%	99.4%	79.7%	88.2%
Case 5	99.2%	99.7%	61.6%	82.7%
Case 6	99.8%	99.9%	93.7%	96.0%
Case 7	99.2%	99.8%	87.3%	96.6%
Case 8	99.8%	99.9%	91.0%	95.3%

TABLE II
SPECIFICITY AND SENSITIVITY VALUES OF BRAIN TUMOR SEGMENTATION USING UNSUPERISED FCM METHOD

	Specificity		Sensitivity	
	Feature Set			
	without deformation	with deformation	without deformation	with deformation
Case 1	100.0%	100.0%	80.6%	81.9%
Case 2	99.2%	99.9%	2.29%	12.47%
Case 3	99.9%	99.9%	22.4%	20.2%
Case 4	98.2%	100.0%	13.8%	18.4%
Case 5	99.9%	99.9%	13.8%	15.7%
Case 6	99.2%	99.5%	11.1%	11.0%
Case 7	97.8%	99.2%	80.3%	84.1%
Case 8	100.0%	100.0%	49.1%	36.5%

By incorporating the relevant lateral ventricular deformation as an additional feature in the feature set for pattern recognition segmentation methods, brain tumor segmentation accuracy increases.

REFERENCES

- [1] Clarke, L.P., Velthuizen, R.P., Camacho, M.A., Heine, J.J., Vaidyanathan, M., Hall, L.O., Thatcher, R.W., Silbiger, M.L.: MRI Segmentation: Methods and Applications. *Neuroanatomy*. 11(3), 343–368 (1995)
- [2] Clark, M., Hall, L., Goldgof, D., Velthuizen, R., Murtagh, F., Silbiger, M.: Automatic Tumor Segmentation Using Knowledge-Based Techniques. *IEEE Trans. Med. Imaging*. 17, 238–251 (1998)
- [3] Ray, N., Greineer, R., Murtha, A.: Using Symmetry to Detect Abnormalities in Brain MRI. *Computer Society of India Communications*. 31(19), 7–10 (2008)
- [4] Saha, B. N., Rayl, N., Greiner, R., Murtha, R., Murtagh, A., Zhang, H.: Quick Detection of Brain Tumors and Edemas: A Bounding Box Method Using Symmetry. *Computerized Medical Imaging and Graphics*. doi:10.1016/j.compmedimag.2011.06.001 (2011)
- [5] Bear, M.F., Connors, B.W., Paradiso, M.A.: *Neuroscience: Exploring the Brain*. Lippincott Williams Wilkins (1996)
- [6] Gunderman, R. B.: *Essential Radiology: Clinical Presentation, Pathophysiology, Imaging*. Thieme Medical Publishers (1998)
- [7] Goetz, C.G., Pappert, E.J.: *Textbook of Clinical Neurology*. W. B. Saunders Company (1999)
- [8] Fix, J.D.: *Neuroanatomy*. Lippincott Williams Wilkins (2001)
- [9] Brown, M., Semeka, R.: *MRI: Basic Principles and Applications*, 3rd Edition. John Wiley and Sons, Inc. (2003)
- [10] The Whole Brain Atlas, <http://www.med.harvard.edu/AANLIB>
- [11] Internet Brain Segmentation Repository provided by MGH CMA. <http://www.cma.mgh.harvard.edu/ibsr>
- [12] Gaser, C., Nenadic, I., Buchsbaum, B.R., Hazlett, E.A., Buchsbaum, M.S.: Deformation-Based Morphometry and Its Relation to Conventional Volumetry of Brain Lateral Ventricles in MRI. *Neuroanatomy*. 13(6), 1140–1145 (2001)
- [13] Chung, S.C., Tack, G.R., Yi, J.H., Lee, B., Choi, M.H., Lee, B.Y., Lee, S.Y.: Effects of Gender, Age, and Body Parameters on the Ventricular Volume of Korean People. *Neurosci. Lett*. 395, 155–158 (2006)
- [14] Prastawa, M., Bullitt, E., Ho, S., Gerig, G.: A Brain Tumor Segmentation Framework Based on Outlier Detection. *Med. Image Anal.* 395, 155–158 (2004)
- [15] Prastawa, M., Bullitt, E., Gerig, G.: Synthetic Ground Truth for Validation of Brain Tumor MRI Segmentation. In: *Proceedings of Medical Image Computing and Computer Assisted Intervention (MICCAI)*, pp.26–33. LNCS, 3749 (2005)
- [16] Louis, D. N., Ohgaki, H., Wiestler, O.D., Cavenee, W.K., Burger, P.C., Jouvet, A., Scheithauer, B.W., Kleihues, P.: The 2007 WHO Classification of Tumors of the Central Nervous System. 114, 97–109 (2007)
- [17] Worth, A.J., Makris, N., Patti, M.R., Goodman, J.M., Hoge, E.A., Caviness, V.S., Kennedy, D.N.: Precise Segmentation of the Lateral Ventricles and Caudate Nucleus in MR Brain Images Using Anatomically Driven Histograms. *IEEE Trans. Med. Imaging*. 17(2):303–310 (1998)
- [18] Wu, Y., Phol, K. Warfield, S.K., Cuttmann, C.R.G.: Automated Segmentation of Cerebral Ventricular Compartments. In: *International Society for Magnetic Resonance in Medicine Eleventh Scientific Meeting and Exhibition*. ISMRM (2003)
- [19] Xiao, K., Ho, S.H., Hassani, A.E.: Automatic Unsupervised Segmentation Methods for MRI Based on Modified Fuzzy C-Means. *Fundamenta Informaticae*. 87(3-4):465–481 (2008)
- [20] Xiao, K., Ho, S.H., Bargiela, A.: Automatic Brain MRI Segmentation Scheme Based on Feature Weighting Factors Selection on Fuzzy C-Means Clustering Algorithms with Gaussian Smoothing. *Int. J. of Comput. Intell. Bioinfo. Sys. Bio*. 1(3):316–331 (2010)
- [21] Zelditch, M., Swiderski, D., Sheets, D.H., Fink, W.: *Geometric Morphometrics for Biologists*. Academic Press (2004)
- [22] Tittgemeyer, M., Wollny, G., Kruggel F.: Visualising Deformation Fields Computed by Non-linear Image Registration. *Comput. Vis. Sci*. 5(1), 45–51 (2002)
- [23] Bookstein, F.L.: Principal Warps: Thin-Plate Splines and the Decomposition of Deformation. *IEEE Trans. Pattern Anal. Mach. Intell.* 11, 567–585 (1989)
- [24] Hajnal, J.V., Hawkes, D.J., Hill, D.G.: *Medical Image Registration*. CRC Press (2001)
- [25] Cover, T.M., Hart, P.E.: Nearest Neighbor Pattern Classification. *IEEE Trans. Inf. Theory*. 13(1), 21–27 (1967)
- [26] Bezdek, J.C., Hall, L.O., Clarke, L.P.: Review of MR Image Segmentation Using Pattern Recognition. *Med. Phys.* 20(4), 1033–1048 (1993)

- [27] Bezdek, J.C.: A Convergence Theorem for the Fuzzy Isodata Clustering Algorithms. *IEEE Trans. Pattern Anal. Mach. Intell.* 2(1), 1–8 (1980)
- [28] Altman, D.G., Bland, J.M.: Statistics Notes: Diagnostic Tests 1: Sensitivity and Specificity. *BMJ.* 308, 1552 (1994)
- [29] Hayes, W.L.: *The Grid: Statistics for the Social Sciences*. Holt, Rhinehart and Winston, New York (1973)
- [30] Everitt, B.S.: Cluster Analysis: a Brief Discussion of Some of the Problems. *The Br. J. Psych.* 147, 143–145 (1972)